Preparation of Chitosan Embedded Recombinant Human Epidermal Growth Factor Nanoparticles as Accelerating Compounds for Skin Remodeling in Chronic Lesions

saadeh hashemi[1], Elnaz Mihandoost,[1], and Sepideh Khaleghi[2]

[1]Islamic Azad University Tehran Medical Sciences
[2]Islamic Azad University

September 5, 2022

Abstract

Chronic lesion has become a major biological burden for individual patients and health organizations. Using nanoparticles as drug delivery systems is remarkable nowadays. The unique properties of chitosan without any toxicity for living creations make it a suitable option for drug delivery. Epidermal growth factor (EGF) is one of the important agents for wound healing, cellular proliferation, extracellular matrix formation, and skin remodeling. A combination of these properties can accelerate the wound healing process. In this study, rh-EGF is embedded into the chitosan nanoparticles by the Ion-gelation method. Nanoparticles are characterized by TEM microscopy and the DLS method and conjugation efficacy is measured by FT-IR radiation. The antibacterial effect of manipulated nanoparticles was estimated by MIC/MBC methods. The cytotoxicity and proliferation were measured by MTT assay on the HFF-1 human fibroblast cell line. Migration assay was accomplished by in vitro scratch model and the gene expression analysis for TGF-β, VEGF, and PDGF were manipulated by the real time-PCR method. The obtained results were considered statistically significant with $P < 0.05$. Obtained results illustrated no toxic effect on the HFF-1 cell line treated with Chitosan-EGF (CS-EGF). In cellular proliferation and migration assays, CS-EGF nanoparticles demonstrated a better effect than free rh-EGF. For the duration of 72h of the experiment, the whole scratch was covered by fibroblasts. The real time-PCR analysis also showed upregulation of all TGF-β, VEGF, and PDGF genes. As CS-EGF nanoparticles in the acceleration of the skin remodeling process showed promising results, subsequent studies might be useful.

Preparation of Chitosan Embedded Recombinant Human Epidermal Growth Factor Nanoparticles as Accelerating Compounds for Skin Remodeling in Chronic Lesions

Saadeh Hashemi[#1], Elnaz Mihandoost[1#], Sepideh Khaleghi[1*]

[1] *Department of Biotechnology, Faculty of Advanced Sciences and Technology, Tehran Medical Sciences, Islamic Azad University, Tehran, Iran.*

[#] Co-first author: Saadeh Hashemi, Elnaz Mihandoost

[*] Corresponding Author: Sepideh Khaleghi, Ph.D., s.khaleghi@iautmu.ac.ir

Acknowledgments

We are grateful to Tehran Medical Sciences, Islamic Azad University for their general support. There is no financial support in this study.

Abstract

Chronic lesion has become a major biological burden for individual patients and health organizations. Using nanoparticles as drug delivery systems is remarkable nowadays. The unique properties of chitosan without

any toxicity for living creations make it a suitable option for drug delivery. Epidermal growth factor (EGF) is one of the important agents for wound healing, cellular proliferation, extracellular matrix formation, and skin remodeling. A combination of these properties can accelerate the wound healing process.

In this study, rh-EGF is embedded into the chitosan nanoparticles by the Ion-gelation method. Nanoparticles are characterized by TEM microscopy and the DLS method and conjugation efficacy is measured by FT-IR radiation. The antibacterial effect of manipulated nanoparticles was estimated by MIC/MBC methods. The cytotoxicity and proliferation were measured by MTT assay on the HFF-1 human fibroblast cell line. Migration assay was accomplished by*in vitro* scratch model and the gene expression analysis for TGF-β, VEGF, and PDGF were manipulated by the real time-PCR method. The obtained results were considered statistically significant with $P < 0.05$.

Obtained results illustrated no toxic effect on the HFF-1 cell line treated with Chitosan-EGF (CS-EGF). In cellular proliferation and migration assays, CS-EGF nanoparticles demonstrated a better effect than free rh-EGF. For the duration of 72h of the experiment, the whole scratch was covered by fibroblasts. The real time-PCR analysis also showed upregulation of all TGF-β, VEGF, and PDGF genes. As CS-EGF nanoparticles in the acceleration of the skin remodeling process showed promising results, subsequent studies might be useful.

Keywords: Chitosan nanoparticles; Epidermal growth factor; Skin lesion; *In vitro* model.

Introduction :

Wound healing is a complex physiological process conducted by a variety of cellular and molecular interactions involving fibroblasts, endothelial cells, keratinocytes, and immune cells which are mediated by essential factors such as growth factors and cytokines. There are four levels of wound healing: hemostasis, inflammation, proliferation, and remodeling. In the initial phase, the onset of hemorrhage in the wound site triggers the platelets. Their degranulation, then, releases alpha granules which cause the abandonment of growth factors such as epidermal growth factor (EGF), platelets-derived growth factor (PDGF), and transforming growth factor-beta (TGF-β). The outcome of this releasing cascade is an influx of inflammatory cells, like neutrophils and macrophages, into the wound site and starting the next phase: inflammation. Within the next 24h neutrophils, macrophages, and lymphocytes influx at the site of injury. They begin to clear debris and bacteria from the wound site to facilitate the next phases of wound healing. In this process, macrophages are the key cells to intricate re-epithelialization, granulation, angiogenesis, and wound contracture.

Among the aforementioned phases, inflammation is an important one in the process of wound healing. Disruptions in this phase, such as infection and poor cellular response, can lead to poor reformation, scar formation, and eventually chronic wounds. The proliferative phase involves capillary budding, extracellular matrix formation, and proliferation and influx of keratinocytes by the migration of the hair follicle stem cells near the leading edge of the wound. Then angiogenesis begins by the vascular endothelial growth factor (VEGF) and some of the fibroblasts differentiate to myofibroblasts to close the wound using their contractile function. Moreover, immature collagen (type III) will also be generated, which has the main role in the perfect appearance of the skin. In the next phase, the type III collagen replaces the type I and the apoptosis of the remaining cells of the previous phase happens (1, 2).

Flagging at the inflammation phase may cause a chronic wound. This problem occurs by systemic and local reasons such as age, obesity, vascular disease, and infection. The main reason for the infection is bacterial colonization in the wound site. Other factors such as diabetes and immunosuppressive disease can turn an acute wound into a chronic ulcer, as well. Arterial and venous leg ulcers, diabetic foot ulcers, pressure ulcers, rheumatologic ulcers and burn ulcers are the most important chronic wound types (3, 4).

Epidermal growth factor (EGF) is a 6-KDa protein that is secreted primarily by platelets, macrophages, and fibroblasts and has a paracrine effect on keratinocytes. It has been confirmed that EGF accelerates the migration of fibroblasts to promote the proliferation phase. EGF expression is upregulated in the initial phases of wound healing. Epidermal Growth Factor Receptors (EGFR) turn on a signaling cascade to promote

cell motility, cellular differentiation, protein secretion, mutagenesis, and apoptosis. Inordinate infiltration of neutrophils causes over-production of ROS, which damages ECM and cell membrane. Moreover, the release of serine protease from neutrophils degrades essential growth factors such as EGF and PDGF. On the other hand, lack of sensation in newborn cells leads to bad localization and down-regulating in EGF receptors. These incidents suggest that although EGF family production is increased, their bio-availability is decreased. Hence, the process of wound healing stops at the inflammatory phase, making the wound a chronic ulcer (1, 5, 6). Certain types of wounds require long-term hospital care where all kinds of nosocomial infections happen. From a molecular point of view, bacterial infection is one of the important reasons for turning an acute wound into a chronic one. Bacterial colonization in the epidermis layer, the presence of matrix metalloproteins in the dermis layer, and abnormal filtration of neutrophils and macrophages, as a result of bacterial infection response, impede the wound healing process in the inflammation phase. Underlying disease and obesity will also make the repair process more difficult (4). In the progression of a chronic wound, bacterial presence in the wound site can lead to an abnormal neutrophil secretion which aims to remove bacterial growth; however, the abandonment of serine proteinase and over-producing reactive oxygen species (ROS) may degrade both ECM and the growth factors. The use of nanomedicine can inhibit bacterial infection while improving the absorption and stability of biological drugs.

Chitosan is a natural linear polysaccharide that is obtained from crustacean shell wastes. The composition of two monomeric units, namely N-acetyl-2-amino-2-deoxy-D-glucose and 2-amino-2-deoxy-D-glucose, make it soluble in acidic solvents, and the β1,4-linkage results in the unbranched structure of this biopolymer (7). *In vivo* and *in vitro* studies on chitosan show no toxic effects on human and animal models (8-10). Its antibacterial effects on gram-negative and gram-positive bacteria (8, 11, 12), hemostatic function (13), and biodegradable properties (14) also make chitosan a suitable choice for dressings and drug delivery. In drug delivery systems based on chitosan nanoparticles, many methods such as emulsion cross-linking, Coacervation-precipitation, spray drying, Emulsion-droplet coalescence, Ionic gelation, Reverse micellar, and Sieving has been developed (8, 15).

Chitosan nanoparticles can accelerate the remodeling phase of the wound healing process by stimulating interleukin 8 (IL-8) secretion from fibroblasts, which results in angiogenesis and migration of neutrophils to the wound site (16). Chitosan also promotes granulation by the proliferation of fibroblasts and enhances neutrophil migration (17, 18). It can decrease scar formation in the re-epithelialization phase as well (17). The ability of chitosan to increase the expression of TGF-β accompanied by collagen production in the early post-injury phase and decreasing TGF-β expression in the last injury phase prevents scar formation and causes better re-epithelialization in the process of wound healing (7, 19).

Time-controlled delivery of drugs is another advantage of chitosan gels, which enhances the treatment process in wound dressing (8, 20). Chitosan can also pass through cellular junctions, subsequently affecting claudin and occludin expression depending on the cell lines and this, in turn, facilitates drug delivery (21, 22). The combination of the growth factor family and chitosan nanoparticles increases the GF family half-life, shows no toxicity and does not affect the expression of interleukin 6 (IL-6) and TNF-α (23).

In the present study, rh-EGF nanoparticles were manipulated by embedding rh-EGF into the chitosan nanoparticles to accelerate the wound healing process, by omitting the infection from the lesion site, and fibroblasts proliferation as migratory and productive cells for rapid treatment. Although chitosan nanoparticles as carriers might prevent scar formation at the end of the remodeling process, using a combination of antibacterial agents with a growth factor from upstream of a healing process cascade makes a proper dressing to avoid chronic lesions.

Materials and Methods

Materials:

Chitosan (CS) (Low molecular weight), Human Recombinant Epidermal Growth Factor (rh-EGF), sodium tripolyphosphate (TPP), and sodium hydroxide (NaOH) were purchased from Sigma Aldrich. Human normal fibroblast cell line (HFF1) for cytotoxicity assay and *Staphylococcus aureus (S. aureus), Bacillus subtilis (B.*

*subtilis), Escherichia coli (E. coli),*and *Pseudomonas aeruginosa (P. aeruginosa)* for antibacterial studies were obtained from Pasture Institute of Iran.

Preparation of CS Nanoparticles:

CS nanoparticles were produced as the result of ionic cross-linking of CS with TPP (24-27). About 1% CS solution was prepared in 20ml of 1% acetic acid followed by adding 2ml of TPP 1% to the aqueous solution while sonicating. Then the solution was stirred for half-hour at room temperature. The final product was obtained by dialyzing in PBS buffer overnight at 4°c temperature.

Preparation of CS-EGF Nanoparticles

About 1% CS become solved in 20ml of 1% acetic acid. 1 mg/ml rh-EGF was added to the solution while stirring at room temperature for 1h, then 2ml of TPP 1% was added to the aqueous solution while sonicating. The dissolved nanoparticles were stirred for 30 minutes at room temperature. The final product was obtained by dialyzing in PBS buffer overnight at 4°c temperature.

Physicochemical Characterization of Nanoparticles

The size and dispersion of nanoparticles were measured by dynamic light scattering (DLS) (28) at 623nm (Scatterscope I, Qudix company, south Korea). The size of particles was further measured by Transmission Electron Microscopy (TEM) and FT-IR spectra of the corresponding nanoparticles were recorded to measure the protein-nanoparticle conjugation (29) (8400S, Shimadzu, Japan).

Determination of Conjugation Efficiency

To purify rh-EGF non-covalent conjugated nanoparticles from free rh-EGF, the ensuing nanoparticles were centrifugated at 14000 rpm for thirty minutes, and then, the absorbent of supernatant was measured at 280nm wavelength to assess the concentration of free rh-EGF. After that, the efficiency of conjugation was calculated by the following equation:

$$\text{The efficiency of conjugation} = \frac{\textit{The concentration of total protein} - \textit{ Concentration of free protein}}{\text{The concentration of total protein}} \times 100$$

In vitro Release Studies of CS-EGF Nanoparticles

In this phase, 1mL of CS-EGF nanoparticles with a concentration of 1 mg/ml was placed in a dialysis sac, with a pore size of 12 KDa, containing PBS buffer (pH 7.4) at 37°c temperature. At the time of the experiment, the dialysis tube was placed in a beaker containing 100 mL of the release medium, maintained at 37^{o}C, and agitated at 80 rpm in a water bath. The samples were then analyzed using a spectrofluorometer and the release profile was observed (30). At different time intervals, 30µL of the medium was removed and replaced with fresh medium. The excitation wavelengths were 342nm with an emission wavelength of 260nm.

Antibacterial Activity Measurement

Antibacterial activity of CS-EGF NPs and CS NPs was assessed against 4 strains, including *Staphylococcus aureus (S. aureus)* and*Bacillus subtilis (B. subtilis)* as gram-positive bacteria, and*Escherichia coli (E. coli)* and *Pseudomonas aeruginosa (P. aeruginosa)* as gram-negative ones, by determining the MIC and MBC concentrations. The prepared nanoparticle, CS and CS-EGF, were added to all 4 groups of bacterial culture medium with 1 mg/ml concentration and the amount of each nanoparticle increased within hours. The results were measured using broth microdilution. The data were obtained by analyzing minimum inhibitory concentration (MIC) and minimum bactericidal concentration (MBC). In each test, an antibiotic was used as a positive control for monitoring the influence of reagent on the growth and mortality of bacteria. In this test, Vancomycin was used as a positive control.

Cell culture

The human HFF-1 normal cell line was purchased from the Pasture Institute of Iran. This cell line was separately cultured in Dulbecco's modified Eagle's medium (DMEM) supplemented with 10% FBS, 2 mM glutamine, 100 µgmL-1 streptomycins, and 100 IU mL-1 penicillin for cellular assessment at 37 °C in a humidified atmosphere of 5% of CO2.

Cell viability and proliferation assay by MTT assessment

Cells were grown in a 96-well culture plate (Corning, NY) containing $15x10^3$ cells in 200 µL of DMEM medium. The cytotoxicity measurement was accomplished with 3-(4, 5-dimethylthiazol-2-yl)-2, 5-diphenyl tetrazolium bromide) (MTT) reagent, as a colorimetric assay, by transforming yellow Tetrazolium to purple. For measuring NPs cytotoxicity, free rh-EGF, CS, and CS-EGF were added to each sample at three frequencies at the concentration of 10µM followed by performing an MTT assay after 24, 48, and 72h. Optical density was measured at 570nm wavelength. Three parallel measurements were carried out for each sample.

Determination of Cellular Migration

To determine cellular migration, the HFF-1 cell line was cultured in 6-well culture plates. Cells were cultured overnight to cover the surface completely. Then, a scratch was made in exact dimensions to make a break between cells. Subsequently, the culture media was limited to the minimum concentration without FBS to prevent the effect of proliferation on the closure of the scratch area. Afterward, free rh-EGF, CS, and CS-EGF samples were added to three different wells at the concentration of 10µM and three wells remained intact as control. After 24h cell migration was observed by invert microscopy of the cell culture.

Gene Expression Studies

Three main genes in the wound healing process, including TGFβ, VEGF, and PDGF, were studied by the Real time-PCR method. After cellular treatment by free rh-EGF, CS, and CS-EGF, the maximum response dose was chosen for determining gene expression (10µM). To extract RNA, Trizol reagent was used (31), with the minimum cell number of one million in each flask. To ensure the purity and quality of the extracted RNA, the wavelength of 260nm and the ratio of 260/280nm were measured using a UV visible-spectrophotometer (BIOTEK). Moreover, the quality assessment of RNA extraction was determined using electrophoresis in agarose gel (2%) and three bands of 28s, 18s, and 5s rRNAs were observed (data not shown). Complementary DNA synthesis was conducted based on the protocols proposed in the BIOFACT kit (BioFACT, Korea). In this method, the reverse transcriptase (RT) enzyme and a mix of oligo (dt) and random hexamer primers were used. Then cDNAs obtained from the treated cell lines were amplified with particular primers of the wound healing genes and the internal control gene (GAPDH). The information related to the sequence and length of the primers and the accession numbers is shown in Table 1. To analyze the data and quantitatively assess gene expression, the Pfaffl method (32) is used to calculate relative gene expression data while accounting for differences in primer efficiencies.

$$Gene\ expression\ ratio = \frac{(E_{\mathrm{GOI}})^{Ct\ GOI}}{(E_{\mathrm{HKG}})^{Ct\ HKG}}$$

Statistical Analysis:

Statistical analysis was accomplished by IBM SPSS V.22.0 (IBM Inc, USA) using a ONE-WAY ANOVA sample and T-test. Values are considered statistically significant with $P < 0.05$.

Results

3.1. Physicochemical Characterization of Nanoparticles:

Nanoparticles of CS and CS-EGF were synthesized by chemical cross-linking with TPP. CS nanoparticles were obtained as a result of the ionic cross-linking between the positively charged protonated amine of chitosan and negatively charged phosphate groups of TPP. By adjusting the concentration of the precursors and stirring speed, the degree of cross-linking and, thus, the particle size will be controlled. CS-EGF nanoparticles were formed using the same mechanism; the positively charged amino groups of chitosan were absorbed into the negatively charged carboxyl groups of EGF-chitosan.

3.1.1. TEM Analysis:

The size and morphology of the prepared nanoparticles were determined using TEM. The absolute diameters of chitosan and EGF-Chitosan nanoparticles were approximately 100±10nm and 100±50nm respectively (Fig. 1A, B).

3.1.2. Particle-size Analysis:

Using dynamic light scattering (DLS) measurements, the size distribution of the 2 types of nanoparticles were obtained. The average hydrodynamic diameter of chitosan and EGF-Chitosan nanoparticles were 150±10nm and 150±50nm respectively (Fig. 1C).

3.2. FT-IR Studies:

Fig. 2 shows the FT-IR spectrum of chitosan and EGF-Chitosan nanoparticles. A characteristic peak at 344.98 cm^{-1}appeared in the infrared spectrum of chitosan, which can be attributed to the –OH groups stretching vibration, and a peek at 1600.97 cm^{-1} for the amide I. Moreover, the spectrum of polysaccharide conjugation of C-O and C-O-C bands is visible at 993.37-1157.33 cm^{-1}. In the EGF-Chitosan spectrum, a peak at 2924.18 cm^{-1} appeared that is related to the conjugation between amino groups of chitosan and phosphates groups of TPP. Also, the 1635.69 cm^{-1} spectrum shows the presence of non-covalent bonds between carboxyl groups of protein and amino groups of chitosan, which indicates chitosan and rh-EGF absorption.

3.3. Conjugation Efficiency Studies:

The primary rh-EGF concentration was 1mg. The protein absorbance was 0.712 at 280nm wavelength associated free protein concentration was 0.324mg with an absorbance of 0.231 at 280nm wavelength. the ultimate conjugation effectivity was calculated at regarding 70% using the subsequent equation:

$$Conjugation\ efficiency = \frac{1 - 0.231}{1} \times 100 = 67\% \simeq 70\%$$

3.4. *In vitro* Release of Embedded EGF CS NPs:

The release profile of EGF-CS NPs in phosphate buffer saline (PBS) under the physiological conditions (pH 7.4 and 37°c temperature) had a releasing rate of 89.3% during the first 24h of the experiment. The results confirmed that the drug release of chitosan nanoparticles follows a time-dependent manner, which is greater in the first 8 hours of the experiment (the main release within 4h was 62.8%, 76.2% in 8h, 85.1% in 16h, and 89.3% in the next 8h respectively).

3.5. Antibacterial Studies:

The antibacterial activity of chitosan and EGF-Chitosan nanoparticles against four different strains of the bacteria was assessed by determining the MIC and MBC values (Table 2). The numbers show the concentration of NPs which had inhibitory and mortality effects on the bacteria during experiments. The zeta potential of CS and EGF-CS NPs were 41±0.25 and 26±0.15 mV respectively. As shown in Table 1, chitosan NPs only possess bactericidal effect on gram-negative and also gram-positive bacteria. Additionally, a higher concentration of EGF-CS NPs had the same effect as the rh-EGF promotes cellular growth further. Obtained results show that EGF-CS NPs have lower inhibitory and bactericidal effects on both gram-negative and gram-positive bacteria. As can be seen, *B. subtilis* from the gram-positive group and*P. aeruginosa* from the gram-negative ones showed more sensitivity against treated NPs while the most resistant spices were *E. coli.*These bacteria also had different behavior toward exposure to EGF-CS and CS NPs regarding mortality, with the MIC level of 24 against 27.4. Principally the MIC range of EGF-CS NP is between 2.53 for *B. subtilis* and 8.5 for *S. aureus* while the MBC range is between 4.75 to 24 µg/ml. CS NP has a MIC range between 1.25 to 7.5 and an MBC range of 3.42 to 27.4. While Vancomycin was used as a positive control, the control did not exhibit any additional harmful effects on bacterial turbidity at the concentration of 0.5% acetic acid.

3.6. Cell Viability and Proliferation Experiments:

Cell viability and proliferation experiments were conducted 24, 48, and 72h after treatment by the concentration of 5, 10, and 15μM of rh-EGF and chitosan NPs in the same concentration of EGF-CS NPs. The results presented 100% viability of controls within 3 days of the experiment. The chitosan NPs enhance cell viability by 90% in the first 24h of incubation. A decrease in cell number after 48 and 72h incubation was observed. There was major growth in cell number in the first 24h after treatment with EGF-Chitosan NPs, which confirm the cellular proliferation duration of the experiment. There is a direct relation between cellular population growth and the increase in the concentration of EGF-CS NPs. The cellular population grew by 144, 162, and 170% within the first 24h of the experiment by the nanoparticle concentration of 5, 10, and 15μM respectively. Within the next 24h of experiments, the rate of cellular growth decreased to 118% for 5 μM, 125% for 10μM, and 142% for 15μM of NP concentrations. In the last 24h of the exposure time (after 72h from the beginning), 145, 162, and 160% of cellular growth rates were observed after being treated with 5, 10, and 15μM of NPs. This outcome may be the result of culture medium shortage as a result of cellular uptake. The last experiment was done by cellular treatment using free rh-EGF, which resulted in 118, 122, and 140% increase in cell number in the first 24h (5, 10, and 15μM of NP exposure). In the next 48h, unusual behavior in the cell number growth was observed, which was 75%, 32%, and 50% decreasing in 5,10 and 15μM concentrations (from 115 to 90%, 118 to 50%, and 120 to 70%), which indicates the short half-life of rh-EGF and the active presence of protease (Fig. 3).

3.7. Cellular Migration Experiments:

Cellular migration is determined by treating the HFF-1 cell line with each of the 3 provided samples (rh-EGF, CS-EGF, and CS). HFF-1 is a human normal fibroblasts cell line that originated from the human foreskin. The treatment solution had a concentration of 10μM of rh-EGF and chitosan NPs, the same concentration of EGF-CS NPs, for 24h. The test was conducted on 12 wells plates and 3 wells remained intact as control. As shown in Fig. 4, there was 50% cellular migration in the first 24h for the sample which was treated by free rh-EGF. The result of treatment using CS NPs showed 20% cellular migration, which is negligible compared to 90±10% cell migration in 24h after being treated using CS-EGF NPs. This significant migration resulted in complete scratch rehabilitation. (Fig. 4).

3.8. Gene Expression Assessments

As discussed above, the best result of cell viability and proliferation experiments was used for real-time PCR and gene expression assessments. The candidate genes were Platelet-derived Growth Factor (PDGF), which regulate cell growth and division, Vascular Endothelial Growth Factor (VEGF), which is a cell signal protein that stimulates the formation of blood vessels, and Transforming Growth Factor beta (TGF-β), which is produced mostly by white blood cells and acts as a multifunctional cytokine. The expression amount of these three genes is really important in the wound healing process and efficient skin remodeling. To assess the influence of manipulated nanoparticles on the gene expression profile of the wound healing process, the best results of cell viability experiments were chosen. The selected concentration was 10μM for free rh-EGF and CS-EGF NPs and 5μM for free chitosan, the same as CS-EGF. Also, the selected duration of the experiment was 24h. According to real-time PCR analysis, there were no significant differences between PDGF, VEGF, and TGF-β gene expression in the HFF-1 cell line after and before exposure to chitosan nanoparticles and the results were very close to the control group. On the other hand, in comparison to the control gene (GAPDH), remarkable elevation was observed in PDGF gene expression of the samples treated with free rh-EGF (Fig. 5A). As shown in Figure 5, as a result of treatment with rh-EGF, PDGF gene expression increased by about 4.2-fold compared to the control group while the expression of PDGF is 7-fold in cells treated with CS-EGF and also 1.5-fold from free rh-EGF treatments. Moreover, the expression of the VEGF gene treated with CS-EGF and rh-EGF reached about 4.2 and 2.8-fold in comparison to the control group, respectively (Fig. 5B). The results also illustrated a 4.5-fold increase in TGF-β gene expression in comparison to the control group and the same difference with chitosan NPs. TGF-β gene expression in cells treated with CS-EGF and rh-EGF is 7 and 3.3-fold relative to the control group, respectively (Fig. 5C). As can be seen in figure 5, EGF-CS NPs are more effective than free rh-EGF of chitosan nanoparticles among

all of the treated cells (Fig. 5).

Discussion

Nowadays, the treatment of a lesion has become a major problem in the healthcare system. Many kinds of diseases such as diabetes, and immunodeficiencies, along with many accidents cause one or more dermal lesions which need treatment. Generally, poor responses to other growth factors, bacterial colonization, poor immune response, collagen degradation, and cellular miss-sensation promote scar formation (1, 2, 5, 6). The role of the Epidermal Growth Factor (EGF) in the treatment of many wound types, involving chronic ones, has already been proven in human and animal studies (33, 34). A systematic review and meta-analysis studies, which were confirmed by clinical trials, demonstrated that the usage of rh-EGF in the cure of chronic ulcers, namely diabetic foot ulcers and burn wounds, was effective (35-37). On the other hand, many studies show the success of using chitosan NPs for wound dressing due to time-controlled drug delivery applications (38), antibacterial effect against gram-positive and negative bacteria (10, 12), and biodegradability without any kind of toxicity to human and animals (19).

In this study, chitosan NPs were manipulated using the Ion-gelation method. Based on previous studies, the Ion-gelation method has been more effective in protein-based drugs for smart drug delivery. A higher concentration of loaded protein encompasses, drug-releasing with a steady speed, weight balancing of the selected drug to the cellular entrance and easy preparation were the reasons for choosing this method instead of the other ones (26). Chitosan chemical reagent provides a high positive surface charge for manipulated nanoparticles across a wide range of pH, which may enhance nanoparticle stability in the acidic wound site. Moreover, preserving the typical shape of polyhedrons as a result of using the NPs is another benefit of TPP (24, 25, 39). TEM and DLS were performed to determine the size range of NPs and the obtained results reported the size of NPs around 150±50nm, as confirmed in past studies on drug delivery uses (40). It is notable that, as discussed above, EGF has a positive charge while it is coated with the negative charges of chitosan. As the result of biochemical cross-linkage of these two different types of particles, the CS-EGF nanoparticle becomes either smaller in size or the same in comparison to free chitosan. The protein release of about 90% on the first day of the experiment in physiological conditions suggests successful nanoparticle manipulation and a steady rate of drug release, in line with previous studies.

Results validate EGF-Chitosan conjugations and the obtained conjugation efficacy was around 70%. Regarding the antibacterial effect of the manipulated nanoparticles, the obtained result demonstrated the lethal effect on both kinds of gram-positive and gram-negative bacteria. As reported in clinical studies, the selected bacterial strain may cause different kinds of bacterial infections and turn an acute wound into a chronic one (6). To overcome bacterial colonization in the wound site, MBC results are more important to cure a chronic wound. However, both CS and CS-EGF NPs showed a greater bactericidal effect on gram-positive species, the CS NPs influence diminished after adding rh-EGF due to a decrease in free amine groups. Although for all the bacteria species involved in the experiments more volume of EGF-CS NPs must be used to overcome bacterial colonization, the *E. coli* strain, which was treated with EGF-CS NPs, may cause a better response for bacterial clearance in this case. However, being exposed to 1 mg/ml of both CS and CS-EGF NPs, the most durable strain was common *E. coli* and the most sensitive one was *B. subtilis* . As shown in the result, it seems that using about 30 µg/ml of each nanoparticle can lead to the demise of all colonies. This hypothesis was approved by the past studies which examined chitosan nanoparticles against *S. aureus* and*E. coli* species. The present study suggests that CS NPs can overcome a wide range of bacteria and also have a wider bactericidal effect (10, 12). As can be seen in cytotoxicity assay results, not only no cytotoxicity was observed against any of the treated nanoparticles on the HFF-1 human fibroblast cell line, but also the proliferation effects were impressive. Moreover, chitosan can increase rh-EGF stability as a protective cover and improve its efficiency during exposure time. Migration assay consequences showed a parallel effect on proliferation. As illustrated in the results section, the wound model treated with manipulated nanoparticles was completely renewed with fibroblasts when treated with EGF-CS NPs. Free chitosan NPs did not show significant success in wound healing during the duration of the experiment. However, the cellular migration was good in the first 24h of free rh-EGF treatment. Although in previous studies rh-EGF protein expo-

sure has resulted in better wound healing, the short half-life of this protein leads to the administration of continuous and higher doses of the drug (36). Improvement of rh-EGF half-life by chitosan NPs might be a better alternative in comparison with free rh-EGF exposure. The ability of chitosan to coat and protect of Epidermal Growth Factor enhances the rh-EGF stability in 3D structure and preserves it from environmental proteases such as Matrix Metalloprotein 9 (MMP9), which increases during the inflammation phase of the wound healing process. Principally the results showed that chitosan nanoparticle has a negligible effect on cellular migration, which can be considered an advantage as uncontrolled cellular migration may cause cellular invasion and lead to poor regeneration and neoplasms in higher concentrations. At the same time, the protective effect of the NP for rh-EGF structure and half-life enhancement make the CS-EGF nanoparticle a suitable choice for accelerating the lesion remodeling process without any side effects. A high level of available rh-EGF can also lead to scar formation, which is a detrimental process in chronic wound healing (1). This can be controlled by the steady speed of chitosan nanoparticles drug release.

On the other hand, there are many studies using lipoid-based nanoparticles as an rh-EGF carriers *in vitro* and *in vivo*for improving the wound healing process (41, 42). There are several studies using hydrogel chitosan dressing to cure diabetic and burn wounds, which confirm the results of this study (43, 44). All of these outcomes advocate the idea that chitosan can enhance the epidermal growth factor effect in the wound dressing process, especially in chronic wounds because of its antibacterial effects. Eventually, the effectiveness of EGF-CS NPs in 72h, shows that it can be used in fewer dosages or even a single dose to enhance the cellular remodeling process in many types of wounds. Other benefits of this treatment method include cost-effectiveness and side effect reduction.

An increase in the growth factors and cytokines leads to better cellular regeneration. In the meantime, the master key of the secretion cascades is EGF, and the main response growth factors are VEGF, PDGF, and TGF-β subsequently. On the other hand, in the case of chronic wounds, a decrease in the level of the aforementioned factors was observed (1). As can be seen in the results, increasing the level of EGF in the wound site may cause overexpression of forgoing genes. In a step-by-step review of the wound healing process in the hemostasis phase, an increase in the amount of EGF, and subsequently PDGF, triggers peripheral cells to divide. Then overexpression of VEGF causes immune cell filtration and TGF-β causes the wound site to enter the inflammatory phase. In the next phase, immune cells, especially macrophages, neutrophils, and lymphocytes, upregulate the expression of TGF-β, which causes the release of the cytokine. PDGF also manages cellular proliferation. Up to this point, there have been no differences in the expression of the desired genes concerning chronic and acute wounds, however, as time goes on, cytokine overload and bacterial existence in the wound site destroy secreted EGF. Therefore, the proliferation phase becomes abnormal. VEGF, which is secreted from fibroblasts, leads to angiogenesis and PDGF consequently causes tissue remodeling. Excessive expression of TGF-β still calls for cytokines that may lead to over-destruction of EGF. After that, the remodeling phase starts with fibroblasts and smooth muscle cells, which secret EGF, PDGF, and TGF-β. In this phase, the existence of EGF leads to damaging the cell apoptosis process and remodeling. A high level of PDGF and TGF-β expression may also lead to cellular mitosis and then scar formation. This can cause an untreated wound, long-term infection, and subsequent problems (5, 6). Since EGF plays an important role in all stages of hemostasis, proliferation, and remodeling, any changes in its concentration lead to poor regeneration. Cytokine degeneration is the reason why they become less bio-available, which can be overcome by adding an exogenic rh-EGF. This enhances the gene expression and results in the prevention of scar formation. Gene expression studies also confirm this hypothesis. Nevertheless, bacterial colonization still possesses a threat in the wound site and can be can overcome by the bactericidal property of chitosan. Adding rh-EGF to wound dressing should also occur in short intervals and continuously due to the short half-life of this protein. Chitosan can overcome this by enhancing rh-EGF efficiency and its stability. Compared with free rh-EGF, the results of chitosan embedded rh-EGF treatment show a more efficient effect on gene expression. Previous studies reported that chitosan also decreases the level of TGF-β in long-term administration and causes ECM formation by accelerating collagen formation, which may reduce the chances of scar generation and speed up recovery (18, 19). Real-time PCR analysis illustrated that by long-term rh-EGF availability the expression of TGF-β, VEGF, and

PDGF remains higher than normal, increasing the efficiency of the wound healing process in different stages.

To summarize, the dual function of CS-EGF NPs can be concluded as the antibacterial effect of chitosan can inhibit bacterial colony formation in the inflammation phase (12) and the effect of rh-EGF on gene expression upregulates the epidermal growth factor receptors (2). As chitosan can pass through the squamosal layer, rh-EGF can be more reachable (45). Moreover, the secretion of vascular endothelial growth factor may be increased by chitosan, which can improve angiogenesis. Subsequently, cell filtration in the wound area may accelerate the hemostasis phase, reducing the time for possible pathogens infection (20). In the next phase, chitosan's existence, as a collagen forming enhancer, and its role in the downregulation of TGF-β in the wound healing process can even completely reduce the chances of scar formation (9). On the other hand, capillary budding, extracellular matrix formation, and keratinocyte migration are considered subsequent effects of rh-EGF. Rh-EGF existence in a wound site can also accelerate degraded cell apoptosis (2). The studies on the effectiveness of rh-EGF as a wound dressing have reached a point that its use in clinical trials is becoming prevalent (37). Although systematic review and meta-analysis proved the rh-EGF effectiveness, elimination of nosocomial infections remains a problem (35, 36). Dextrin-rhEGF also shows a better result than free rh-EGF in diabetic wound cures (33). The histological evaluation in a mouse model of wound healing, which was treated by hydrogel embedded polymer-growth factor conjugated nanoparticles, confirmed the obtained results of the current study regarding cell viability and proliferation in the wound sites (34), except not considering the genes involved in this process.

1. **Conclusions**This study confirmed the fact that using chitosan nanoparticles as a carrier for epidermal growth factors in an *in vitro* model for dressing a chronic wound can accelerate the cellular remodeling and eradicate the concern of bacterial infection in the process of treatment. The superiority of the manipulated nanoparticle in this study is the slow release of the epidermal growth factor, bactericidal effect, collagen formation, passing through the cell layer, thermo-sensitivity, biodegradability, and harmlessness for organisms. The improvement in rh-EGF half-life makes these CS-EGF NPs a suitable choice for chronic wound dressing.
2. **Conflict of Interest**The authors declare no conflict of interest.
3. **References**

1. Barrientos S, Stojadinovic O, Golinko MS, Brem H, Tomic-Canic MJWr, regeneration. Growth factors and cytokines in wound healing. 2008;16(5):585-601.

2. Gantwerker EA, Hom DBJCips. Skin: histology and physiology of wound healing. 2012;39(1):85-97.

3. Morton LM, Phillips TJJJotAAoD. Wound healing and treating wounds: differential diagnosis and evaluation of chronic wounds. 2016;74(4):589-605.

4. Powers JG, Higham C, Broussard K, Phillips TJJJotAAoD. Wound healing and treating wounds: Chronic wound care and management. 2016;74(4):607-25.

5. Grazul-Bilska AT, Johnson ML, Bilski JJ, Redmer DA, Reynolds LP, Abdullah A, et al. Wound healing: the role of growth factors. 2003;39(10):787-800.

6. Zhao R, Liang H, Clarke E, Jackson C, Xue MJIjoms. Inflammation in chronic wounds. 2016;17(12):2085.

7. Anitha A, Sowmya S, Kumar PS, Deepthi S, Chennazhi K, Ehrlich H, et al. Chitin and chitosan in selected biomedical applications. 2014;39(9):1644-67.

8. Agnihotri SA, Mallikarjuna NN, Aminabhavi TMJJocr. Recent advances on chitosan-based micro-and nanoparticles in drug delivery. 2004;100(1):5-28.

9. Patrulea V, Ostafe V, Borchard G, Jordan OJEJoP, Biopharmaceutics. Chitosan as a starting material for wound healing applications. 2015;97:417-26.

10. Anitha A, Rani VD, Krishna R, Sreeja V, Selvamurugan N, Nair S, et al. Synthesis, characterization, cytotoxicity and antibacterial studies of chitosan, O-carboxymethyl and N, O-carboxymethyl chitosan

nanoparticles. 2009;78(4):672-7.

11. Felt O, Carrel A, Baehni P, Buri P, Gurny RJJoOP, Therapeutics. Chitosan as tear substitute: a wetting agent endowed with antimicrobial efficacy. 2000;16(3):261-70.

12. Vaz JM, Pezzoli D, Chevallier P, Campelo CS, Candiani G, Mantovani DJCpd. Antibacterial coatings based on chitosan for pharmaceutical and biomedical applications. 2018;24(8):866-85.

13. Janvikul W, Uppanan P, Thavornyutikarn B, Krewraing J, Prateepasen RJJoaps. In vitro comparative hemostatic studies of chitin, chitosan, and their derivatives. 2006;102(1):445-51.

14. Patois E, Cruz SOd, Tille JC, Walpoth B, Gurny R, Jordan OJJoBMRPAAOJoTSfB, The Japanese Society for Biomaterials,, et al. Novel thermosensitive chitosan hydrogels: In vivo evaluation. 2009;91(2):324-30.

15. Grenha AJJodt. Chitosan nanoparticles: a survey of preparation methods. 2012;20(4):291-300.

16. Ueno H, Mori T, Fujinaga TJAddr. Topical formulations and wound healing applications of chitosan. 2001;52(2):105-15.

17. Howling GI, Dettmar PW, Goddard PA, Hampson FC, Dornish M, Wood EJJB. The effect of chitin and chitosan on the proliferation of human skin fibroblasts and keratinocytes in vitro. 2001;22(22):2959-66.

18. Ueno H, Yamada H, Tanaka I, Kaba N, Matsuura M, Okumura M, et al. Accelerating effects of chitosan for healing at early phase of experimental open wound in dogs. 1999;20(15):1407-14.

19. Baxter RM, Dai T, Kimball J, Wang E, Hamblin MR, Wiesmann WP, et al. Chitosan dressing promotes healing in third degree burns in mice: gene expression analysis shows biphasic effects for rapid tissue regeneration and decreased fibrotic signaling. 2013;101(2):340-8.

20. Chupa JM, Foster AM, Sumner SR, Madihally SV, Matthew HWJB. Vascular cell responses to polysaccharide materials:: in vitro and in vivo evaluations. 2000;21(22):2315-22.

21. Piazzini V, Landucci E, D'Ambrosio M, Fasiolo LT, Cinci L, Colombo G, et al. Chitosan coated human serum albumin nanoparticles: A promising strategy for nose-to-brain drug delivery. 2019;129:267-80.

22. Anandhakumar S, Krishnamoorthy G, Ramkumar K, Raichur AJMS, C E. Preparation of collagen peptide functionalized chitosan nanoparticles by ionic gelation method: An effective carrier system for encapsulation and release of doxorubicin for cancer drug delivery. 2017;70:378-85.

23. Rajam M, Pulavendran S, Rose C, Mandal AJIjop. Chitosan nanoparticles as a dual growth factor delivery system for tissue engineering applications. 2011;410(1-2):145-52.

24. Bhumkar DR, Pokharkar VBJAP. Studies on effect of pH on cross-linking of chitosan with sodium tripolyphosphate: a technical note. 2006;7(2):E138-E43.

25. Gan Q, Wang T, Cochrane C, McCarron PJC, Biointerfaces SB. Modulation of surface charge, particle size and morphological properties of chitosan–TPP nanoparticles intended for gene delivery. 2005;44(2-3):65-73.

26. Gan Q, Wang TJC, Biointerfaces SB. Chitosan nanoparticle as protein delivery carrier—systematic examination of fabrication conditions for efficient loading and release. 2007;59(1):24-34.

27. Qi L, Xu Z, Jiang X, Hu C, Zou XJCr. Preparation and antibacterial activity of chitosan nanoparticles. 2004;339(16):2693-700.

28. Pecora RJJonr. Dynamic light scattering measurement of nanometer particles in liquids. 2000;2(2):123-31.

29. Frey BL, Corn RMJAC. Covalent attachment and derivatization of poly (L-lysine) monolayers on gold surfaces as characterized by polarization- modulation FT-IR spectroscopy. 1996;68(18):3187-93.

30. Alemdaroğlu C, Değim Z, Celebi N, Zor F, Oztürk S, Erdoğan D. An investigation on burn wound healing in rats with chitosan gel formulation containing epidermal growth factor. Burns : journal of the International Society for Burn Injuries. 2006;32(3):319-27.

31. Peirson SN, Butler JN. RNA Extraction From Mammalian Tissues. In: Rosato E, editor. Circadian Rhythms: Methods and Protocols. Totowa, NJ: Humana Press; 2007. p. 315-27.

32. Pfaffl MWJNar. A new mathematical model for relative quantification in real-time RT–PCR. 2001;29(9):e45-e.

33. Hardwicke JT, Hart J, Bell A, Duncan R, Thomas DW, Moseley RJJocr. The effect of dextrin–rhEGF on the healing of full-thickness, excisional wounds in the (db/db) diabetic mouse. 2011;152(3):411-7.

34. Hajimiri M, Shahverdi S, Esfandiari MA, Larijani B, Atyabi F, Rajabiani A, et al. Preparation of hydrogel embedded polymer-growth factor conjugated nanoparticles as a diabetic wound dressing. 2016;42(5):707-19.

35. Zhang Y, Wang T, He J, Dong JJIwj. Growth factor therapy in patients with partial-thickness burns: a systematic review and meta-analysis. 2016;13(3):354-66.

36. Bui TQ, Bui QVP, Németh D, Hegyi P, Szakács Z, Rumbus Z, et al. Epidermal Growth Factor is Effective in the Treatment of Diabetic Foot Ulcers: Meta-Analysis and Systematic Review. 2019;16(14):2584.

37. Esquirol-Caussa J, Herrero-Vila EJJoDT. Human recombinant epidermal growth factor in skin lesions: 77 cases in EPItelizando project. 2019;30(1):96-101.

38. Garg U, Chauhan S, Nagaich U, Jain NJApb. Current advances in chitosan nanoparticles based drug delivery and targeting. 2019;9(2):195.

39. Gadkari RR, Suwalka S, Yogi MR, Ali W, Das A, Alagirusamy RJCp. Green synthesis of chitosan-cinnamaldehyde cross-linked nanoparticles: Characterization and antibacterial activity. 2019;226:115298.

40. Rawal T, Mishra N, Jha A, Bhatt A, Tyagi R, Panchal S, et al. Chitosan Nanoparticles of Gamma-Oryzanol: Formulation, Optimization, and In vivo Evaluation of Anti-hyperlipidemic Activity. 2018;19:1894-907.

41. Değim Z, Çelebi N, Alemdaroğlu C, Deveci M, Öztürk S, Özoğul CJIwj. Evaluation of chitosan gel containing liposome-loaded epidermal growth factor on burn wound healing. 2011;8(4):343-54.

42. Gainza G, Pastor M, Aguirre JJ, Villullas S, Pedraz JL, Hernandez RM, et al. A novel strategy for the treatment of chronic wounds based on the topical administration of rhEGF-loaded lipid

nanoparticles: In vitro bioactivity and in vivo effectiveness in healing-impaired db/db mice. 2014;185:51-61.

43. Choi JS, Yoo HSJJoBMRPA. Pluronic/chitosan hydrogels containing epidermal growth factor with wound-adhesive and photo-crosslinkable properties. 2010;95(2):564-73.

44. Yoo Y, Hyun H, Yoon S-J, Kim SY, Lee D-W, Um S, et al. Visible light-cured glycol chitosan hydrogel dressing containing endothelial growth factor and basic fibroblast growth factor accelerates wound healing in vivo. 2018;67:365-72.

45. Föger F, Schmitz T, Bernkop-Schnürch AJB. In vivo evaluation of an oral delivery system for P-gp substrates based on thiolated chitosan. 2006;27(23):4250-5.

Tables

gene	Forward/Reverse	Sequence	Sequence	Produc
PDGF	F	5´CGTGCGTGACATTAAAGAGAA3´	5´CGTGCGTGACATTAAAGAGAA3´	135
	R	5´CGCTCATTGCCGATAGTGAT3´	5´CGCTCATTGCCGATAGTGAT3´	
TGF-ß	F	5´AAGGCCTGGTCTGGGAGTAT3´	5´AAGGCCTGGTCTGGGAGTAT3´	149

gene	Forward/Reverse	Sequence	Sequence	Produc
	R	5´ GCATCCACTCGCTCACTACA3´	5´ GCATCCACTCGCTCACTACA3´	
VEGF	F	F	5' CTGGAGCGTGTACGTTGGT 3'	179
	R	R	5' CGTTTAACTCAAGCTGCCTCG 3'	
GAPDH	F	5´ CGTAAGGATTGCATCGGACT3´	5´ CGTAAGGATTGCATCGGACT3´	138
	R	5´ AGGGGGACTAAGGAGGTGAA3´	5´ AGGGGGACTAAGGAGGTGAA3´	

Table 1. Forward and reverse primers sequences of PDGF, *TGF-ß* and VEGF genes for gene expression analysis by real-time PCR assay.*GAPDH* gene was used as control.

Treatments	Particle size (nm)	Zeta Potential (mV)	Concentration (mg/ml)	MIC/MBC (µg/ml)	MIC/MBC (µg/ml)	MIC/MBC (µg/ml)	MIC/MBC (µg/ml)
				Gram-Positive bacteria S. aureus	Gram-Positive bacteria B. subtilis	Gram Negative bacteria E. coli	Gram Negative bacteria P. aeruginosa
EGF-C-TPP	147±10	26±0.15	1 mg/ml	8.5/15.5	2.53/4.75	11.4/24	3.28/7.10
C-TPP	126±10	41±0.25	1 mg/ml	6.5/13.6	1.25/3.42	7.5/27.4	1.74/6.5

Table 2. The antibacterial activity of CS-EGF and CS was assessed against four different strains by determining the MIC and MBC values. While Vancomycin was used as a positive control, the control did not exhibit any additional harmful effects on bacterial turbidity at the concentration of 0.5% acetic acid.

Figures

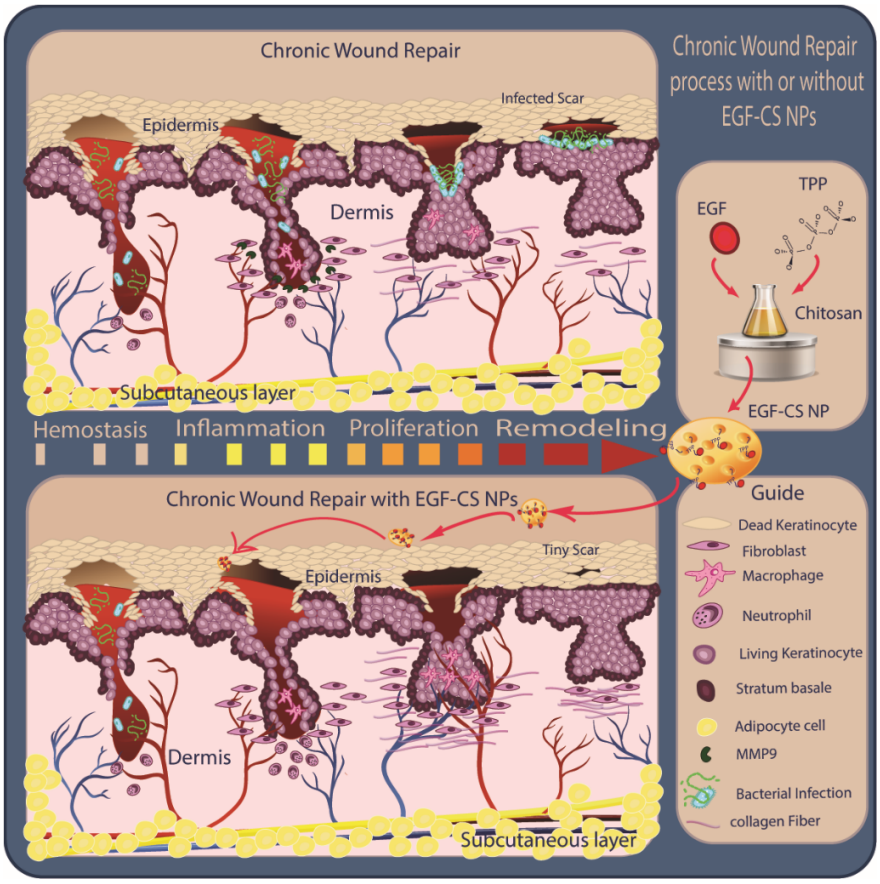

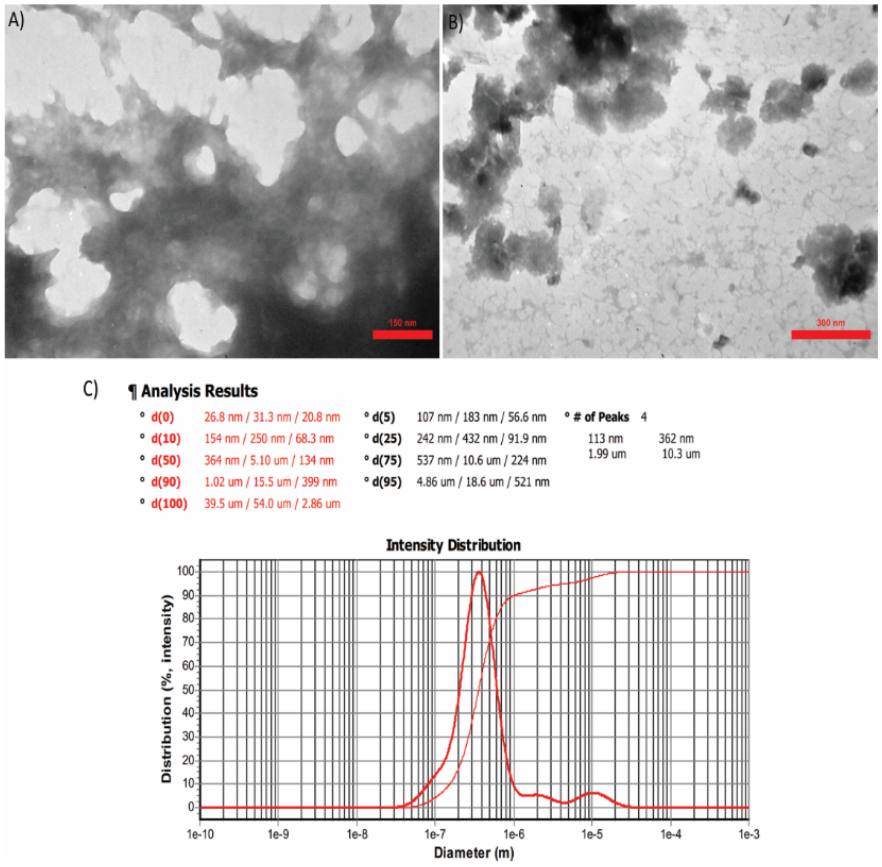

Figure 1. Topological characterization of nanoparticles. A) Transmission electron microscopy results of chitosan nanoparticles. The absolute diameters of chitosan nanoparticles were around 100±10nm. B) TEM microscopy of rh-EGF chitosan nanoparticles had particle diameters of around 100±50nm. C) The result of measuring the size of the conjugated nanoparticles with rh-EGF protein using the DLS method and its analysis.

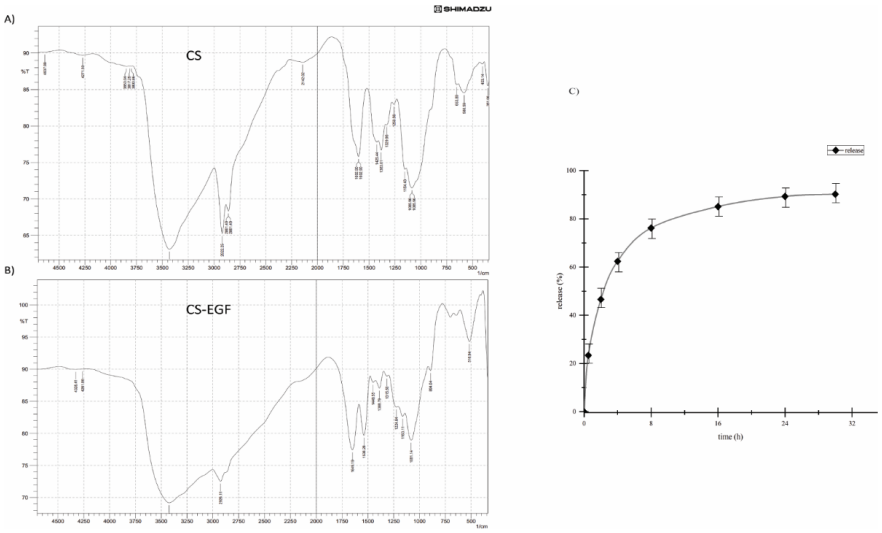

Figure 2. Physicochemical characterization and drug release of manipulated nanoparticles. A) The FTIR spectrum of free chitosan nanoparticles and B) Chitosan nanoparticles conjugated with rh-EGF protein. The 1635.69 cm-^{1} spectrum shows the non-covalent bonds between carboxyl groups of the protein and amino groups of chitosan, which indicates the difference between two groups of nanoparticles, showing the connection between chitosan and rh-EGF in CS-EGF nanoparticles. C) CS-EGF NPs drug release profile, measured at 0, 4, 8, 16, 24, and 30h of the experiment and T=37±1 *C, pH 7.4.

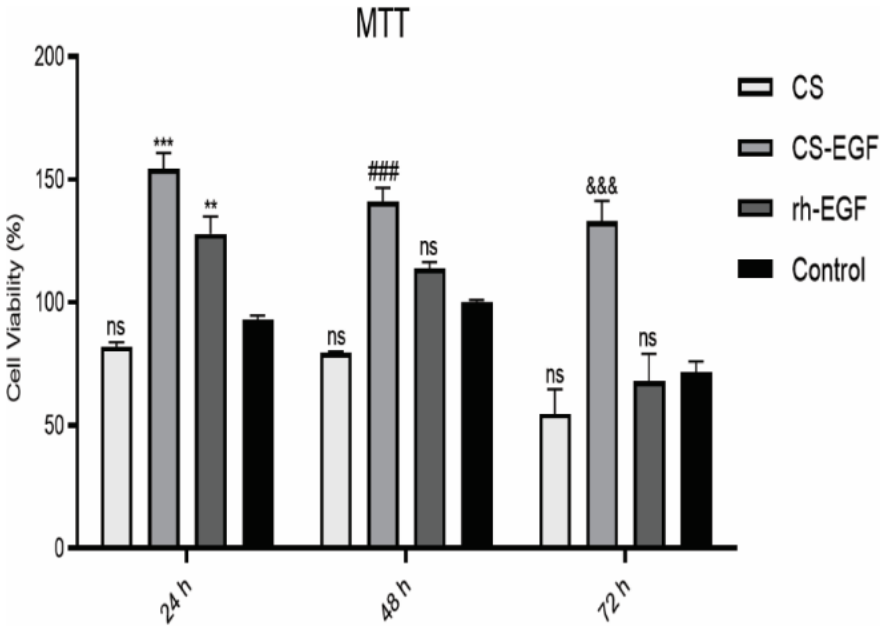

Figure 3. The diagram of cell viability assay at 24, 48, and 72 hours by MTT method. Empty chitosan samples did not show a significant difference after 24, 48, and 72 hours. This increase can be seen after 48 and 72 hours, however, after 72 hours rh-EGF protein has decreased significantly, which is due to protein instability after 3 days.

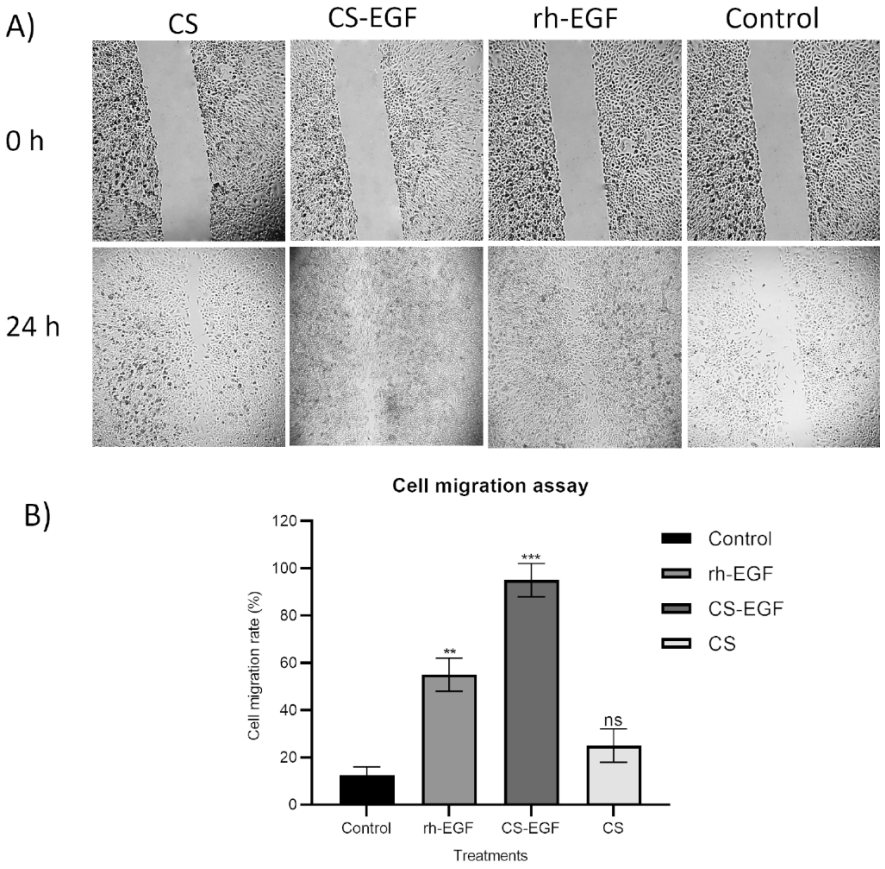

Figure 4. A) The evaluation of cell proliferation after 24, 48, and 72 hours at different concentrations of 5, 10, and 15μM for rh-EGF protein, 60, 120, and 180 μl for non-conjugated chitosan nanoparticles, and 5, 10, and 15μM for nanoparticles conjugated with rh-EGF protein with an optical microscope. B) Cell migration rate diagram which illustrates a 5-time increase against the control group for the cells that were treated with CS-EGF.

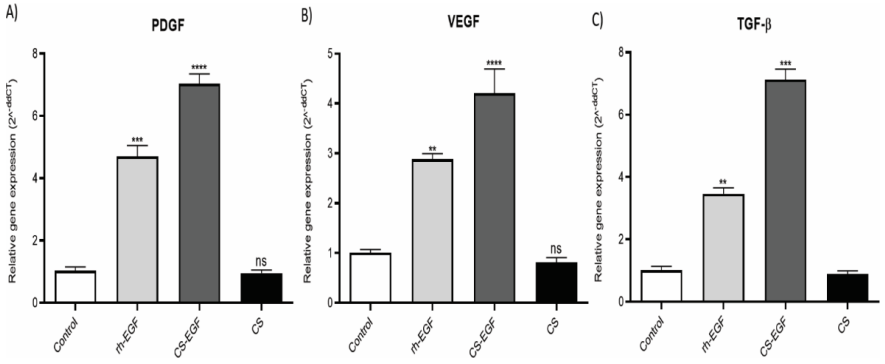

Figure 5. Real-time PCR analysis results showed that treatment with rh-EGF protein results in an over-expression of PDGF, VEGF, and TGF-β genes. A, B, and C diagrams are related to PDGF, VEGF, and TGF-β gene expressions respectively. The results show no significant changes in the expression level of the aforementioned gene treated with free chitosan. When treated with EGF-CS NPs, a higher expression level of the three intended genes has been observed.

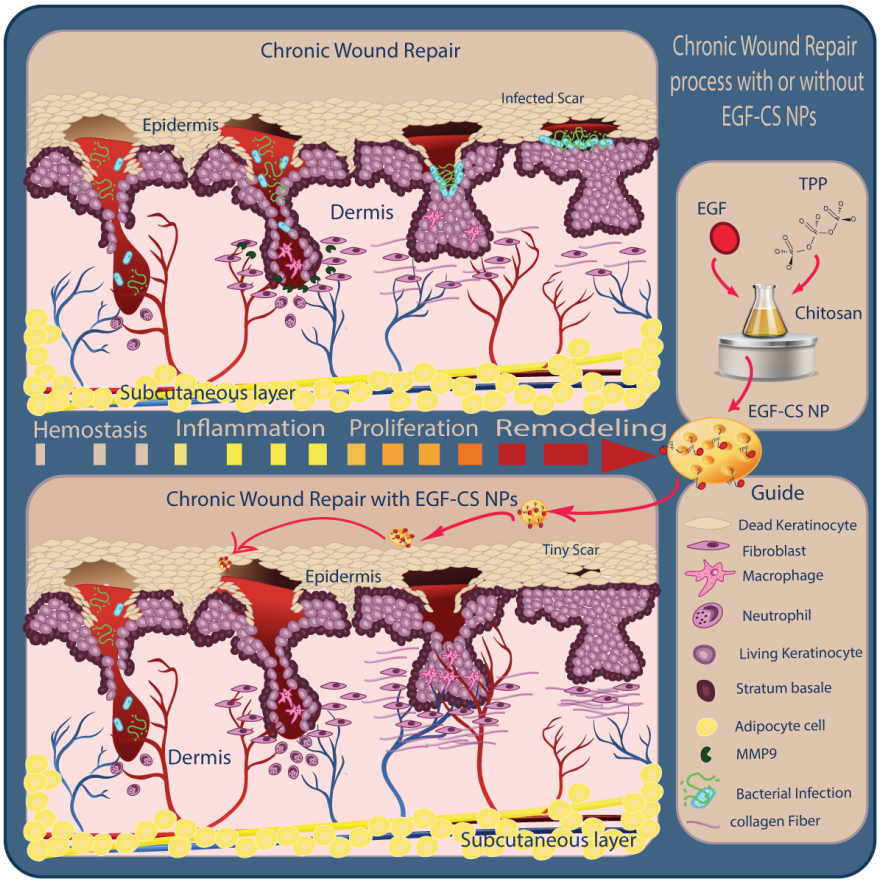

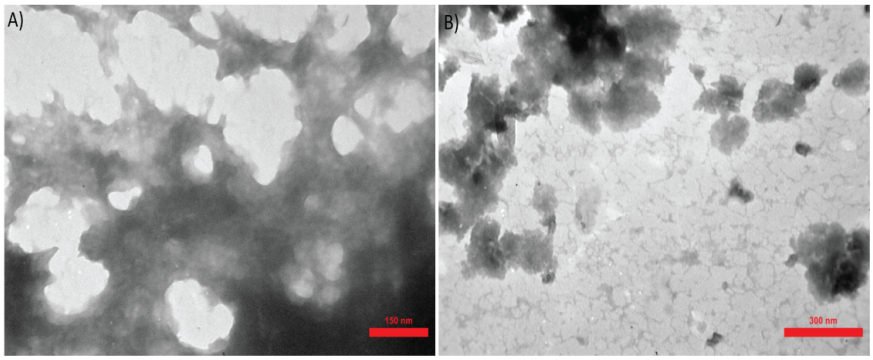

C)

¶ Analysis Results

° **d(0)**	26.8 nm / 31.3 nm / 20.8 nm	° **d(5)**	107 nm / 183 nm / 56.6 nm	° **# of Peaks**	4
° **d(10)**	154 nm / 250 nm / 68.3 nm	° **d(25)**	242 nm / 432 nm / 91.9 nm	113 nm	362 nm
° **d(50)**	364 nm / 5.10 um / 134 nm	° **d(75)**	537 nm / 10.6 um / 224 nm	1.99 um	10.3 um
° **d(90)**	1.02 um / 15.5 um / 399 nm	° **d(95)**	4.86 um / 18.6 um / 521 nm		
° **d(100)**	39.5 um / 54.0 um / 2.86 um				

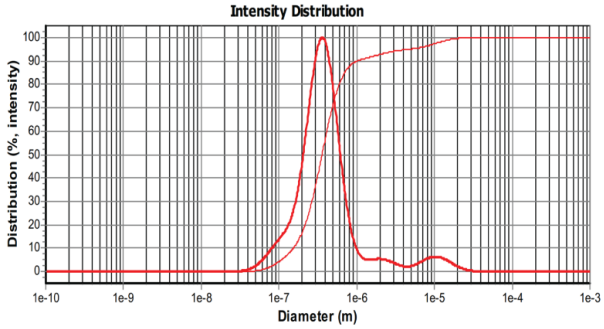

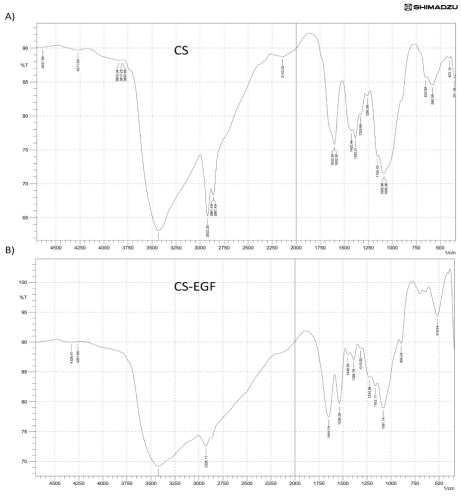

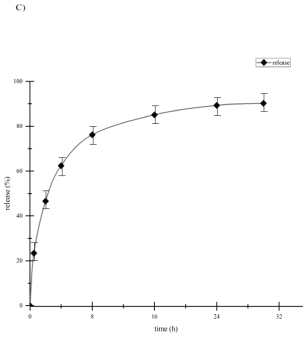

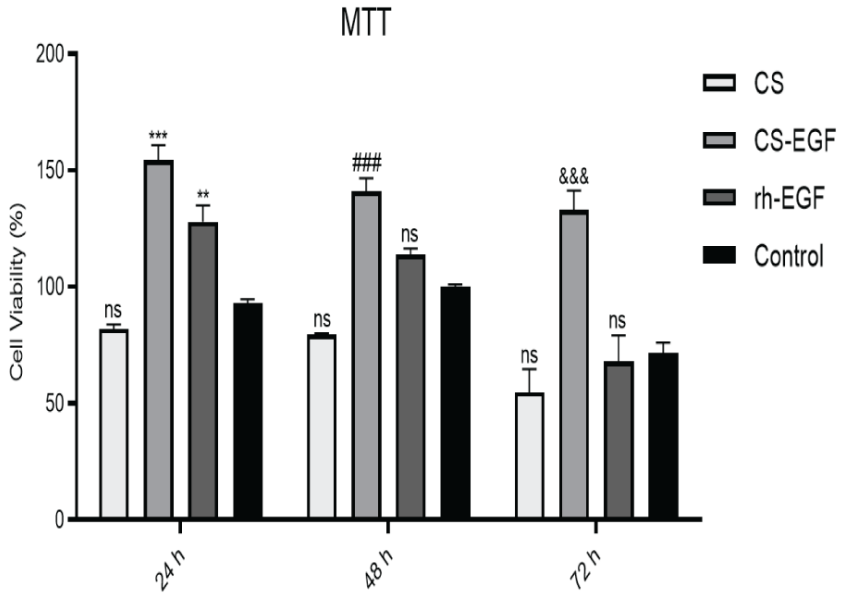

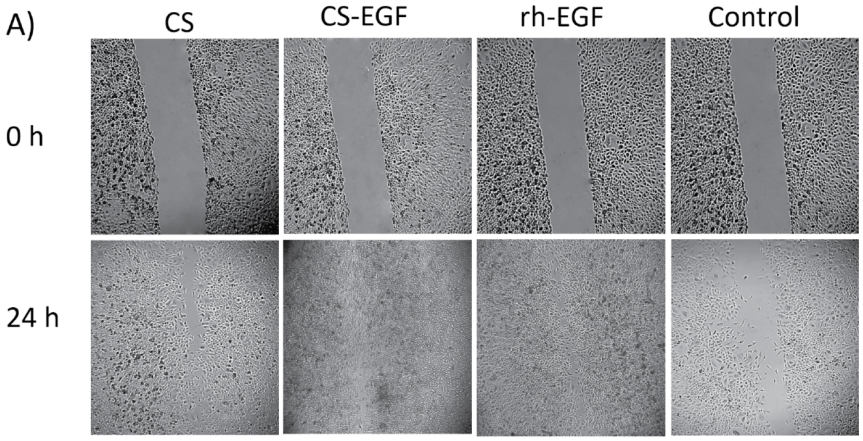

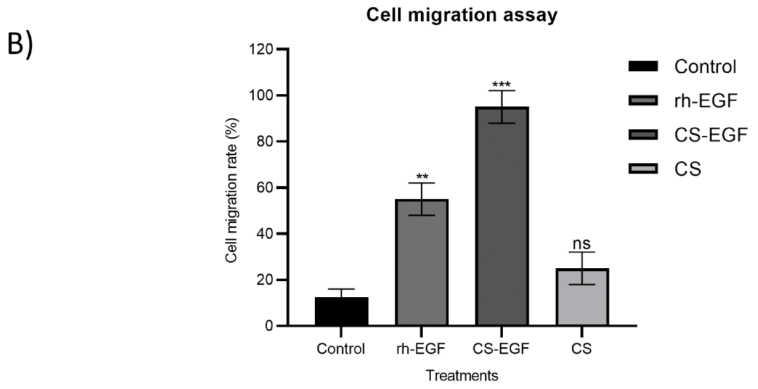

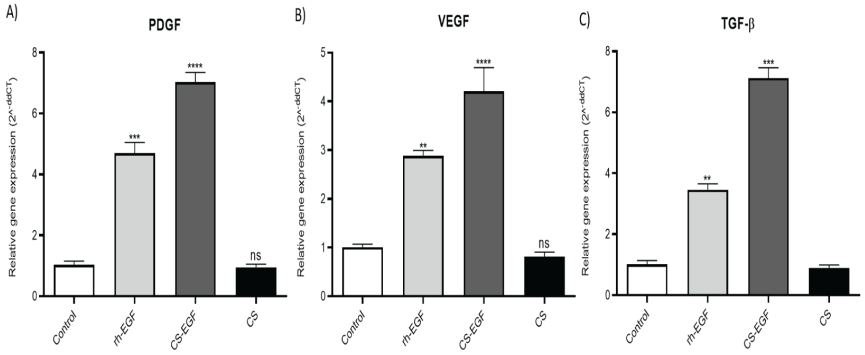

Hosted file

table 1.docx available at https://authorea.com/users/505891/articles/584826-preparation-of-chitosan-embedded-recombinant-human-epidermal-growth-factor-nanoparticles-as-accelerating-compounds-for-skin-remodeling-in-chronic-lesions

Hosted file

table 2.docx available at https://authorea.com/users/505891/articles/584826-preparation-of-chitosan-embedded-recombinant-human-epidermal-growth-factor-nanoparticles-as-accelerating-compounds-for-skin-remodeling-in-chronic-lesions